Catalysis Letters 48 (1997) 31–38

Metal–support interactions during the CO_2 reforming of CH_4 over model TiO_x / Pt catalysts

Michael C.J. Bradford and M. Albert Vannice*

Department of Chemical Engineering, The Pennsylvania State University, University Park, PA 16802-4400, USA

Received 25 April 1997; accepted 12 August 1997

To obtain insight into the importance of metal–support interactions (MSI) in the CO_2 reforming of CH_4, the reaction was studied using pure TiO_2, high-purity Pt powder, and two model TiO_x/Pt systems. The latter two TiO_x/Pt catalysts, prepared by oxidation of Ti nonylate deposited on the Pt powder surface, contained either one ($\theta = 1$) or ten ($\theta = 10$) theoretical monolayers of TiO_2. The H_2 and CO chemisorption capacities showed respective decreases of 1/3 and 1/2 on the latter two catalysts although the N_2 BET surface areas were essentially unchanged. XRD analysis of either TiO_x/Pt sample detected no TiO_x structures. Specific rates (μmol/(s g_{cat})), areal rates (μmol/(s m^2)) and turnover frequencies (s^{-1}) for the CO_2 reforming of CH_4 decreased in the order TiO_x/Pt ($\theta = 10$) TiO_x/Pt ($\theta = 1$) $\gg$ Pt powder > TiO_2. Neither pure Pt powder nor pure TiO_2 showed appreciable activity for CH_4–CO_2 reforming; thus the dramatic increase in activity is attributed to the creation of new sites in the metal–support interfacial region which promote CH_4 dissociation, CO_2 dissociation and reduction, and subsequent CH_xO decomposition. In addition, temperature-programmed hydrogenation of used catalyst samples clearly showed that TiO_x overlayers on the Pt surface suppress carbon deposition during reaction via an ensemble effect, thus improving activity maintenance.

Keywords: methane, carbon dioxide, CO_2 reforming, platinum, titania, metal–support interactions

1. Introduction

Due to the strong thermodynamic potential for carbon formation during the CO_2 reforming of CH_4 at low temperatures and equimolar feed ratios, a catalyst which kinetically inhibits carbon deposition is required [1]. Previous investigations of the CO_2 reforming of CH_4 on supported Ni [1,2], Pt [3], Ir [4], and Rh [5,6] have indicated that the support utilized can be important for determining both catalyst activity and resistance to carbon deposition. For example, various groups have shown that properly prepared NiO–MgO solid solutions exhibit stable activity and resistance to carbon deposition [1,7–9]. Although the precise reasons for this are not known, it has been speculated that both electronic and structural factors are important. For example, it has been suggested that formation of a NiO–MgO solid solution decreases the donor ability of the Ni particles, thereby inhibiting both CO disproportionation [8] and CH_4 activation [1]. Additionally, the structural stability of Ni particles in NiO–MgO solid solutions, as evidenced by the high degree of difficulty of reduction [10], should prevent both Ni sintering and carbon diffusion into Ni crystallites, thereby suppressing filamentous carbon growth [1]. Similarly, Chen and Ren have clearly shown that the formation of $NiAl_2O_4$ in a Ni/Al_2O_3 catalyst during pretreatment greatly suppresses carbon deposition [11].

It has also been shown in the literature that Ni/TiO_2 [1], Pd/TiO_2 [12], Rh/TiO_2 [5,6], Pt/TiO_2 [3], and Ni/La_2O_3 [2] exhibit suppressed carbon deposition during CO_2–CH_4 reforming. Based on temperature-programmed oxidation and hydrogenation as well as chemisorption results, this behavior has been attributed to the decoration of metal particle surfaces by either TiO_x or LaO_x species which geometrically destroy large ensembles of metal atoms that serve as active sites for carbon deposition [1–3]. In addition, it has been proposed that sites at the metal–support interface may promote catalyst activity [1,3,5,13]. To simultaneously probe the role of TiO_x overlayers and the influence of the metal–support interface on carbon deposition and kinetic activity during the CO_2 reforming of CH_4, model TiO_x/Pt catalysts were prepared and characterized using chemisorption, X-ray diffraction, DRIFTS and temperature-programmed hydrogenation, and their kinetic behavior was determined.

2. Experimental

The UHP Pt powder (Alfa Aesar, 99.999%) used in this study contained 3 ppm Pd and 7 ppm Rh as impurities. Two model TiO_x/Pt catalysts were prepared by (i) adding 3 g of Pt powder to a solution of titanium(IV) nonylate ($Ti(C_9H_{19}O)_4$) dissolved in 6 cm^3 of *n*-pentane, (ii) continuously stirring and evaporating the *n*-pentane, and (iii) calcining in flowing air (470 sccm) at 673 K for 2 h [14]. These two catalysts contained either one (0.003 g $Ti(C_9H_{19}O)_4$/g Pt) or ten (0.028 g $Ti(C_9H_{19}O)_4$/g Pt)

---

* To whom correspondence should be addressed.

theoretical monolayers of TiO_2 and are thus designated as TiO_x/Pt ($\theta = 1$) and TiO_x/Pt ($\theta = 10$), respectively. TiO_2 (Degussa P-25, 47 m^2/g) alone was also studied as a reference.

All H_2 and CO chemisorption experiments were performed at 300 K in a stainless steel volumetric apparatus following reduction at either 723 or 773 K. The N_2 BET isotherms were obtained at 77 K with the same apparatus immediately following CO adsorption experiments. The Pt powder was calcined in flowing O_2 ($O_2/He = 1/4$) for 1 h at 673 K for cleaning and subsequently reduced in flowing H_2 at 723 K for 1 h [14]. After evacuation for 30 min at 723 K, the catalyst was cooled under vacuum (ca. 10^{-7} Torr) to room temperature. The TiO_x/Pt ($\theta = 1$) and TiO_x/Pt ($\theta = 10$) catalysts were reduced for 1 h at 773 K following a procedure described previously for supported Pt catalysts [3].

This 773 K reduction procedure was also used for all catalysts prior to kinetic evaluation in a high-temperature reactor system described previously [1]. The amount of catalyst used during these experiments, ca. 100 mg, was chosen to maintain differential conditions with respect to gas-phase concentrations, which were typically less than 5% CH_4 conversion. All activity tests were carried out under ca. 740 Torr absolute pressure, with a feed composition of $CO_2/CH_4/He = 1/1/1.8$ and a total feed flow rate of 20 sccm (WHSV = 12,000 $cm^3\ g^{-1}\ h^{-1}$) over a temperature range of 673 K to 773 K.

Temperature-programmed hydrogenation (TPH) was utilized to investigate carbonaceous deposits on used catalyst samples. After termination of reaction, the catalyst was purged with He and cooled overnight to room temperature. The following day the temperature was ramped at a rate of 10 ± 1 K/min from 298 to 1073 K, while a 50% mixture of hydrogen in helium was passed through the catalyst bed at atmospheric pressure. This procedure has been described previously [3].

X-ray diffraction (XRD) was performed with a Rigaku Geigerflex system using filtered Cu $K\alpha$ radiation and was used to identify bulk phases in the reduced catalyst samples. For Pt powder, the long-range order was estimated using the Pt(111) and Pt(200) reflections and the Scherrer formula with Warren's correction for instrumental line broadening [15].

An N_2-purged FTIR spectrometer (Mattson Instruments, RS-10000) equipped with a DRIFTS cell (Harrick Scientific, HVC-DR2) and a praying mantis mirror assembly (Harrick Scientific, DRA-2C0) was used to study CO and CO_2 adsorption as well as in situ CO_2–CH_4 reforming on Pt powder between 300 and 723 K. Spectra were obtained from 750 to 4000 cm^{-1} with a resolution of 4 cm^{-1}. To study irreversible CO adsorption, flowing CO was passed over Pt powder at 300 K for 15 min, followed by purging in a He/Ar mixture to remove gas-phase and reversibly adsorbed CO. Both CO_2 adsorption and CO_2–CH_4 reforming were studied between 300 and 723 K with gas-phase CH_4 and CO_2 present.

3. Results

A summary of the N_2 BET surface areas, chemisorption uptakes, and Pt crystallite sizes determined for each catalyst is provided in table 1. Based on an average of all three N_2 BET measurements, the Pt crystallite size is estimated to be (± standard deviation) about 670 ± 20 nm, or about 18 times larger than that estimated by line-broadening analysis of the Pt(111) and Pt(200) reflections. Because XRD is a bulk technique sensitive to long-range order, the estimated d_v values are indicative of an average shorter-range order presumably caused by grain boundaries and shear planes within the large Pt particles. Thus, from the data in table 1 the mean crystallite order within the Pt powder particles is estimated to be 38 ± 3 nm; however, XRD line broadening becomes quite insensitive for large crystallites. The Pt lattice parameter estimated from the XRD spectra for Pt powder, TiO_x/Pt ($\theta = 1$) and TiO_x/Pt ($\theta = 10$) was $a_0 = 3.925 \pm 0.001$ Å, in agreement with the value of 3.923 Å for bulk Pt [16].

Table 1
Surface area (S), chemisorption and estimated crystallite size of Pt catalysts

Catalyst	S [a] (m^2/g)	H_2 uptake [c] ($\mu mol/g_{cat}$)		CO uptake [d] ($\mu mol/g_{cat}$)		Crystallite size (nm)	
		U_{irr}	U_{tot}	U_{irr}	U_{tot}	d_s [a]	d_v [e]
Pt powder	0.42 (0.38) [b]	2.2	3.8	3.7 ± 0.1	4.1	670	36
TiO_x/Pt ($\theta = 1$)	0.40	1.4	2.6	2.6 ± 0.2	3.0	700	42
TiO_x/Pt ($\theta = 10$)	0.43	0.8	1.9	2.4 ± 0.2	2.8	650	36
TiO_2 powder	47	–	–	–	–	–	–

[a] Estimated using an N_2 molecular surface area of 0.162 nm^2.
[b] Value in parentheses based on total H_2 uptake assuming $H/Pt_s = 1$ and 1.2×10^{19} Pt_s/m^2 [48].
[c] Values obtained by extrapolation to $P_{H_2} = 0$ Torr.
[d] Obtained at 100 Torr CO.
[e] From XRD line-broadening analysis of Pt(111) and Pt(200) reflections.

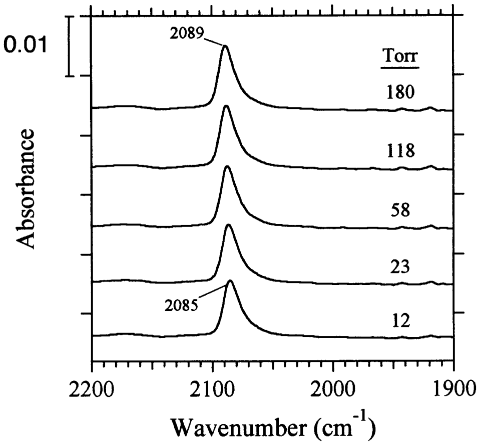

Figure 1. DRIFTS spectra of irreversible CO adsorption at 300 K on reduced Pt powder at various CO pressures (referenced to spectrum of reduced Pt powder at 300 K prior to gas admission).

DRIFT spectra of CO adsorbed on Pt powder under 12 to 180 Torr clearly show only one band which shifts from 2085 to 2089 cm^{-1} with increasing coverage (figure 1). These are the wavenumbers associated with CO chemisorbed to a Pt surface atom with a coordination number of 9.0 ± 0.2 [17], indicating that the exposed Pt surface is principally Pt(111), as expected for bulk Pt because the (111) surface is most densely packed and has the lowest surface free energy [18]. Based on a Pt powder surface area of 0.42 m^2/g and a site density of 1.2×10^{19} Pt_s/m^2, the saturation surface coverage of hydrogen atoms, θ_H, and CO, θ_{CO}, can be calculated from the total adsorption uptakes (table 1) to be 0.91 and 0.49, respectively. The latter value is in good agreement with the value of $\theta_{CO} = 0.5$ on Pt(111) at 300 K reported by Ertl et al. [19], indicating that the chosen pretreatment procedure provided a clean Pt surface.

Although the total surface areas of TiO_x/Pt ($\theta = 1$) and TiO_x/Pt ($\theta = 10$) do not differ substantially from that of the Pt powder, the irreversible chemisorption capacities decreased by 33 ± 3% and 50 ± 14%, respectively, implying that uniform coverage was not attained and that three-dimensional TiO_x structures formed on the Pt powder surface. XRD spectra of the TiO_x/Pt ($\theta = 1$) and TiO_x/Pt ($\theta = 10$) catalysts, however, were identical to that of Pt powder and revealed no additional reflections (figure 2), indicating that either the TiO_x structures were amorphous or their concentration was below the detection limit of the diffractometer.

After about 5 h on stream, the catalysts were purged with He and cooled to room temperature overnight under flowing He. On the Pt powder, TiO_x/Pt ($\theta = 1$), and TiO_x/Pt ($\theta = 10$) catalysts, CH_4 formation during TPH was observed only above 700 K and thus is attributed to hydrogenation of surface carbon (figure 3). With all three catalysts the peak maximum observed at 920–950 K is in agreement with prior TPH studies of SiO_2- and Cr_2O_3-supported Pt [3]. The amount of carbon deposition on each catalyst, as determined via integration of the CH_4 evolution spectra, gave C/Pt_{surf} ratios of 31 for Pt powder, 14 for TiO_x/Pt ($\theta = 1$), and 10 for TiO_x/Pt ($\theta = 10$), indicating that TiO_x species on the Pt surface diminish the amount of carbon deposited during reaction. Supra-monolayer coverages of carbon have been observed previously during CO_2–CH_4 reforming over noble metals [20]; however, carbon deposition on the titania surface may also occur.

Carbon deposition on the Pt surface during reaction can be inhibited by the presence of TiO_x species on the Pt

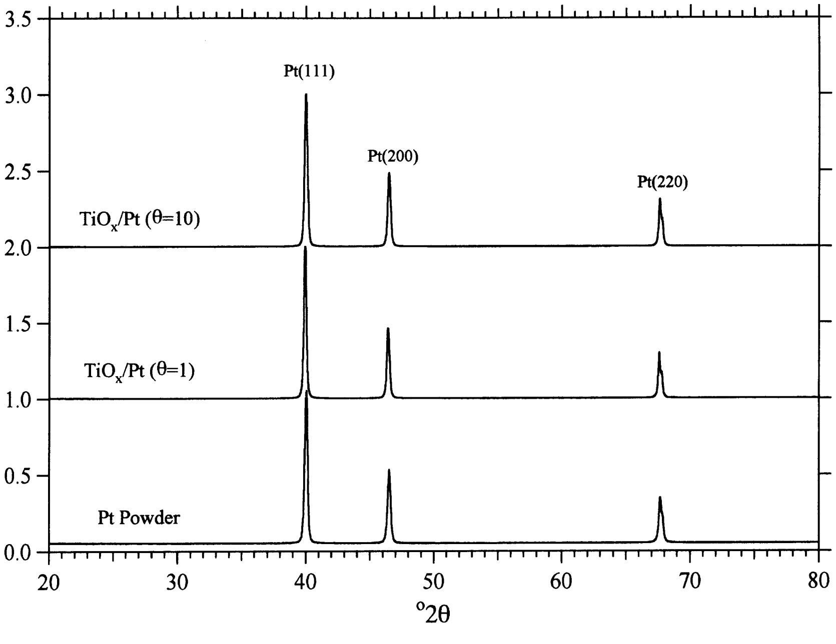

Figure 2. Indexed XRD spectra of Pt powder, TiO_x/Pt ($\theta = 1$) and TiO_x/Pt ($\theta = 10$).

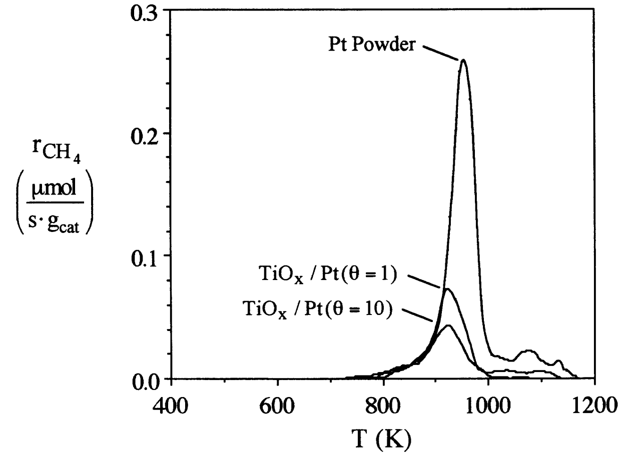

Figure 3. CH_4 evolution during TPH of used TiO_x/Pt ($\theta = 10$), TiO_x/Pt ($\theta = 1$) and Pt powder catalysts: $\beta = 10$ K/min.

surface via an ensemble effect because large ensembles of atoms are required for both CH_4 dissociation and CO disproportionation [3]. If active sites for CO_2–CH_4 reforming are associated only with Pt atoms, then the partial coverage of the Pt surface by TiO_x species should inhibit both carbon deposition *and* the rate of CH_4–CO_2 reforming; however, both areal (μmol/(s m^2)) and specific (μmol/(s g_{cat})) rates as well as the turnover frequencies (TOF) for these catalysts, based on the irreversible CO uptake at 300 K, show clearly that this is not the case (see table 2). The nomenclature used for the aforementioned rate basis is that recently used by Boudart [21]. The order of initial catalyst activity – TiO_x/Pt ($\theta = 10$) > TiO_x/Pt ($\theta = 1$) ≫ Pt powder > TiO_2 – is independent of basis, as indicated in table 2, and provides strong evidence to support the contention that active sites for the CO_2 reforming of CH_4 are created in the metal–support interfacial region.

The variation in activity for TiO_x/Pt ($\theta = 10$) and TiO_x/Pt ($\theta = 1$) at 723 K and Pt powder at 823 K is shown in figure 4. During the period of 30 to 200 min time on stream, Arrhenius runs were performed, and these results are shown in figure 5. A linear deactivation rate ($\delta r/\delta t$) of 24 ± 1%/h (0.40 ± 0.02%/min) at 823 K was observed for Pt powder at the end of the Arrhenius run, i.e., during 240 to 320 min on stream (figure 4), in excellent agreement with the linear deactivation rate of 23 ± 3%/h observed previously for Pt/SiO_2 at 723 K [3]. Linear deactivation of the two TiO_x-promoted catalysts was not observed, but plots of the reaction rate ($-r$) at 723 K versus ln(time on stream) were linear, i.e., $r = a + b\ \ln(t)$, where a and b are constants. For these two catalysts, time-dependent deactivation rates ($\delta r/\delta t = \delta(b \ln(t))/\delta t = b/t$) of 14%/$t$(min) for TiO_x/Pt ($\theta = 1$) and 16%/t(min) for TiO_x/Pt ($\theta = 10$) were obtained. In an effort to correct the Arrhenius data for deactivation and estimate the apparent activation energy, the observed rates of deactivation were utilized assuming that they were approximately independent of temperature; thus, due to the relatively large rates of deactivation much uncertainty is associated with the apparent activation energies obtained for these catalysts (see table 2 and figure 5). Nevertheless, the values obtained for Pt powder are in good agreement with those obtained for SiO_2- and Cr_2O_3-supported Pt [3]. Also, despite significant initial rates of deactivation for the two TiO_x/Pt catalysts, it is clear that after substantial time on stream, both TiO_x/Pt catalysts deactivate less rapidly than Pt powder, even though the conditions for carbon deposition are more favorable.

DRIFT spectra after CO_2 adsorption on Pt powder at 293 K reveal two bands at 2068 and 2075 cm^{-1} for linearly adsorbed CO on Pt, indicating that CO_2 dissociation occurs (figure 6A). As the temperature increases, the surface coverage of CO due to CO_2 dissociation, as indicated by the integral optical density of adsorbed CO, initially increases then finally decreases. Gas-phase CO formation, indicated by broad rotational bands on either side of the observed minimum at 2143 cm^{-1}, begins at about 623 K. DRIFT spectra during CO_2–CH_4 coadsorption at 293 K (figure 6B) show a marked increase in the optical density of adsorbed CO compared to CO_2 adsorption alone, implying that CH_4 promotes the dissociation of CO_2, as observed with Rh [6]. Although formation of gas-phase CO is observed during CO_2–CH_4 coadsorption and reaction as the temperature increases, the amount of adsorbed CO on the surface is comparatively much less than during CO_2 adsorption alone at high temperatures. Carbonaceous fragments resulting

Table 2
Initial, maximum catalyst activity at 723 K and apparent activation energies

Catalyst	Conversion (%)		Activity				E_{app} (kcal/mol)				
	CH_4	CO_2	(μmol CO/(s g_{cat}))	(μmol CO/(s m^2))	TOF_{CO} [a] (s^{-1})	TOF_{CH_4} [a] (s^{-1})	CH_4	CO_2	CO	H_2	H_2O
TiO_x/Pt ($\theta = 10$)	4.6	9.0	5.1	12	2.1	0.71	5	5	5	b	b
TiO_x/Pt ($\theta = 1$)	3.7	7.0	4.0	10	1.5	0.52	7	8	8	8	8
Pt powder	0.35 ± 0.05	0.60 ± 0.08	0.44 ± 0.18	1.0	0.1	0.04	17.5	17.5	17.5 ± 0.5	22	13
TiO_2	0.1	0.2	0.21 ± 0.13	0.005	–	–	b	b	b	b	b

[a] Calculated by normalizing specific activity (μmol/(s g_{cat})) to irreversible CO adsorption (μmol/g_{cat}).

[b] Not possible to accurately measure.

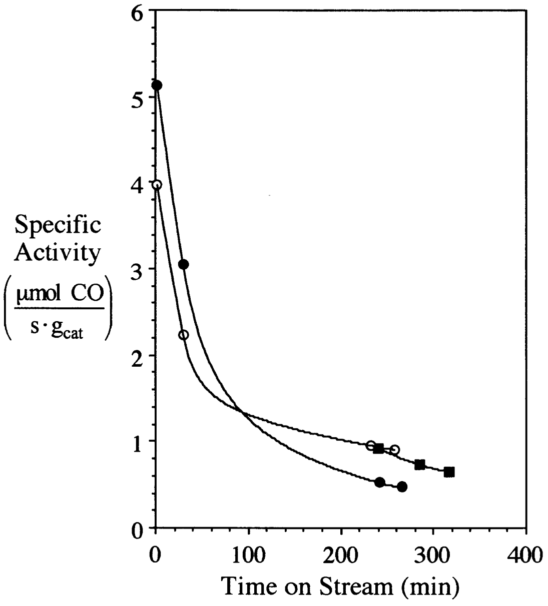

Figure 4. Activity maintenance of: (■) Pt powder at 823 K, (○) TiO_x/Pt ($\theta = 1$) at 723 K and (●) TiO_x/Pt ($\theta = 10$) at 723 K during CO_2–CH_4 reforming. Arrhenius runs were conducted between 30 and 200 min time on stream (see figure 5). Reaction conditions: $CH_4/CO_2/He = 1/1/1.8$, $P = 1$ atm, WHSV = 12,000 cm^3 h^{-1} g^{-1}.

from CH_4 decomposition at higher temperatures may block adsorption sites for CO; consequently, CH_4 decomposition may be the primary source of inactive carbon deposition during reaction.

DRIFT spectra after CO_2 adsorption on TiO_x/Pt ($\theta = 10$) at 293 K reveal two bands at 2078 and 2086 cm^{-1} for linearly adsorbed CO on Pt, as shown in figure 7. The observed shift of 10 cm^{-1} in the symmetric CO vibration relative to that of CO adsorbed on Pt powder (see figure 5A), indicates a strengthening of the CO bond and perhaps a decrease in the CO heat of adsorption in the presence of TiO_x species on the Pt surface. This is consistent with the calorimetric results of Herrmann et al. who showed that TiO_x species on Pt decrease the average CO heat of adsorption by about 5 kcal/mol [22]; however, it could also imply a decrease in dipolar interactions due to the reduction in site density caused by the TiO_x species. An increase in temperature resulted in a gradual vibrational shift to lower wavenumbers for adsorbed CO and the formation of gas-phase CO, as observed during CO_2 adsorption on Pt powder. Upon introduction of CH_4 at 723 K, the intensity of gas-phase CO increased while the intensity of adsorbed CO vanished, in agreement with the prior suggestion that carbon deposits resulting from CH_4 decomposition block sites for CO adsorption.

4. Discussion

The aforementioned TPH results in figure 3 and the activities listed in table 2 clearly indicate that TiO_x species on the Pt surface not only decrease the amount of carbon deposition during CO_2–CH_4 reforming, most likely via an ensemble effect, but also create active sites, presumably in the metal–support interfacial region. This conclusion is consistent with previous results obtained with Pt dispersed on SiO_2, Cr_2O_3, ZrO_2 and TiO_2 [3]; however, there is an unexpected result in the present investigation that requires an explanation, i.e., the initial specific activity of Pt powder is one-tenth that of Pt/SiO_2, Pt/Cr_2O_3 or Pt/ZrO_2 [3]. The absence of any detectable adsorbed CO on Pt powder under reforming conditions suggests that a carbonaceous overlayer may rapidly form on the Pt powder surface and physically block most of the surface Pt atoms; however, the possibility must also be considered that the low TOF of Pt powder may be a consequence of structure sensitivity associated with CO_2 reforming of CH_4. The TOFs of 1.5 and 2.1 s^{-1} obtained at 723 K for the two TiO_x-promoted

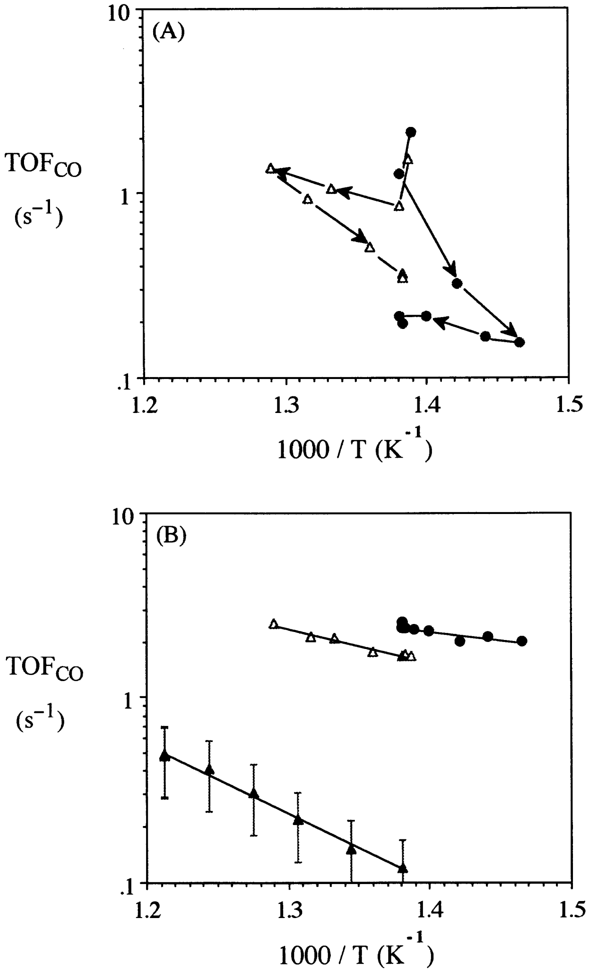

Figure 5. Arrhenius plots of turnover frequencies for CO production (A) prior to correction, where the arrow indicates the sequence of data collection, and (B) after correction for deactivation: (●) TiO_x/Pt ($\theta = 10$), (△) TiO_x/Pt($\theta = 1$), and (▲) Pt powder. Reaction conditions: $CH_4/CO_2/He = 1/1/1.8$, $P = 1$ atm, WHSV = 12,000 cm^3 h^{-1} g^{-1}.

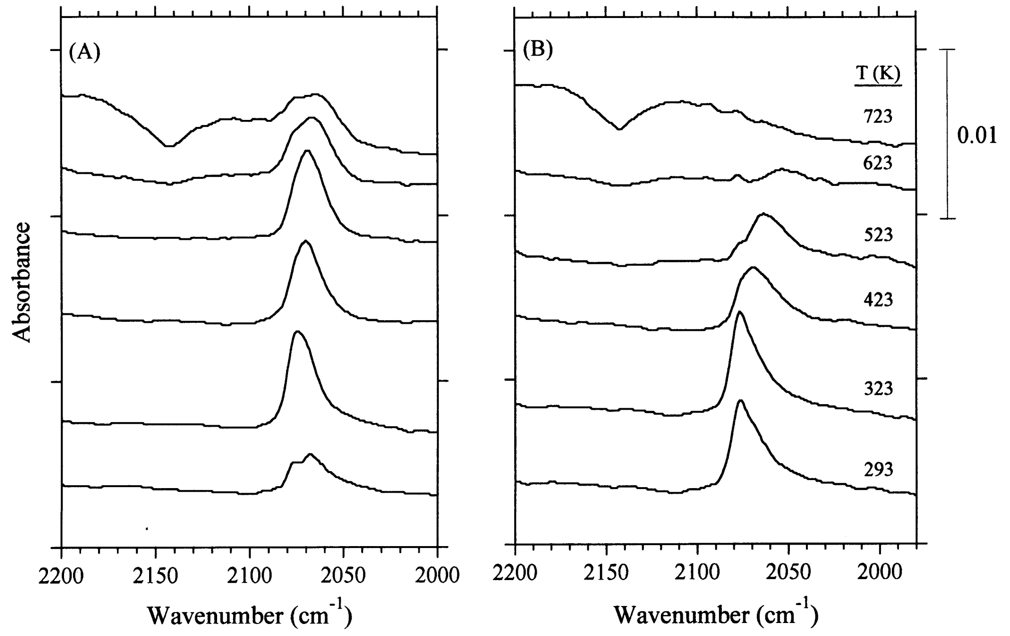

Figure 6. DRIFT spectra during (A) CO_2 adsorption ($CO_2/Ar = 1/5$) and (B) CH_4–CO_2 reforming ($CH_4/CO_2/Ar = 1/1/4$) on Pt powder at different temperatures (referenced to spectrum of reduced Pt powder at corresponding temperature prior to gas admission): total $P = 1$ atm.

catalysts are consistent with the TOF of 4.9 s^{-1} obtained at 723 K for a supported Pt/TiO_2 catalyst [3]. Comparatively, the TOF of 0.94 s^{-1} for Pt/SiO_2 [3] is only 2 to 5 times smaller; thus, the intrinsic rate enhancement by TiO_x is relatively small. This aspect, coupled with the large amount of carbon deposition on pure Pt powder, provides strong evidence that the low rate for the CO_2–CH_4 reforming over Pt powder is a consequence of rapid, initial carbon deposition.

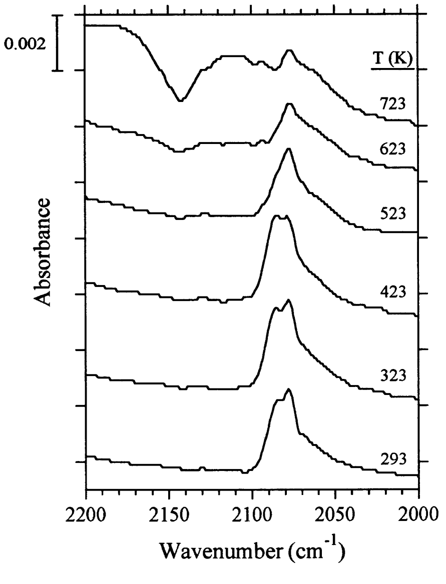

Figure 7. DRIFT spectra during CO_2 adsorption ($CO_2/Ar = 1/5$) on TiO_x/Pt ($\theta = 10$) at different temperatures (referenced to spectrum of reduced TiO_x/Pt ($\theta = 10$) at corresponding temperature prior to CO_2 admission): total $P = 1$ atm.

The possibility that the reactions associated with the CO_2 reforming of CH_4 over Pt may be structure sensitive cannot be discounted. For example, it has been shown that the electrochemical reduction of CO_2 with H_2 to yield CO and H_2O via the reverse water–gas shift (RWGS) reaction is slower on Pt(111) than on either Pt(100) or Pt(110), and that CO_2 reduction is enhanced by the presence of surface defects [23,24]. CO_2 hydrogenation over carbon-supported Pt has also been reported to be structure sensitive [25]. Scattering experiments related to CO_2 adsorption on Pt(111) have shown that CO_2 undergoes with equal probability either direct inelastic scattering or trapping and desorption (with an estimated heat of adsorption of 5 kcal/mol), i.e., there is no detectable dissociation [18]. The general observations are that both CO_2 dissociation and reduction are difficult on Pt(111), and that surface defects promote activity on the Pt(111) surface. This hypothesis may explain the result reported by Prichard and Hinshelwood in 1925 that CO_2 is activated on only a small fraction of the Pt surface during the RWGS reaction on a Pt wire [26]. An early report by Somorjai et al. concluded that the dissociation of diatomic molecules and the breaking of C–C and C–H bonds can be structure sensitive over Pt surfaces [27], and Beebe et al. have shown that the dissociation probability of CH_4 on Ni surfaces is structure sensitive, with the probability increasing in the order Ni(111)<Ni(100)<Ni(110) [28]. Thus, by analogy, it may be that CH_4 activation over Pt is also structure sensitive, as indicated by the gas-phase interaction between

CH_4 and Pt clusters [29]. Despite the evidence in the literature indicating that CO_2 dissociation and reduction is structure sensitive on Pt surfaces, the RWGS is extremely rapid over supported Pt catalysts [3]. This can be attributed to highly dispersed Pt particles which are expected to have a significant number of corner and edge atoms, as illustrated by model calculations [30], and the rapid hydrogenation of CO_2 in the presence of a support [3]. Furthermore, two studies in the literature have addressed the structure sensitivity of CO_2–CH_4 reforming over a noble metal. Zhang et al. reported that the initial TOF for Al_2O_3- and TiO_2-supported Rh is a function of Rh particle size, implying structure sensitivity [5], whereas Mark and Maier found that the TOF on Rh is independent of both support and metal particle size, indicating structure insensitivity [31]. A comparison of six different Rh/SiO_2 catalysts, including the two aforementioned, has shown only a four-fold variation in the TOF for CH_4 disappearance as the dispersions varied from 0.08 to unity [32]. This argues against the CO_2–CH_4 reforming reaction being structure sensitive, at least over Rh/SiO_2 under the reaction conditions utilized. Consequently, although the much lower activity of Pt powder, with primarily (111) planes, for CO_2–CH_4 reforming is possibly due in part to inhibition of both CH_4 and CO_2 dissociation, thus also making CO_2 dissociation or reduction a kinetically slow step on Pt powder, the possibility of rapid deactivation due to carbon deposition seems more likely, and remains as a very reasonable explanation for the lower activity on large Pt crystallites.

The promotion of activity by the addition of TiO_x to the Pt powder surface is presumably due in part to the promotion of both CH_4 dissociation and CO_2 dissociation and reduction. Tanaka et al. showed using XPS that TiO_x promotes CO_2 dissociation on Pt(111) at temperatures as low as 77 K [33], and Fancheng et al. reported that TiO_x promotes CH_4 decomposition at room temperature [34]. Recent results with TiO_2-supported Pt indicate that lattice oxygen may participate in the activation of both CH_4 and CO_2 at elevated temperatures [3]. It has also been suggested that interfacial sites in TiO_x/Pt catalysts could promote decomposition of CH_xO intermediates, one of the proposed slow kinetic steps in CH_4–CO_2 reforming over supported Pt catalysts [3]. In this regard, the possible role of Ti^{3+} centers at the metal–support interface can be addressed. Reduction of Pt/TiO_2 at 773 K (HTR) has been shown by XPS [33,35,36], IR spectroscopy and ESR [37], and EPR [38] to induce partial reduction of TiO_2 to create Ti^{3+} species, and Benneviot and Haller deduced that some Ti^{3+} centers reside at the Pt–TiO_2 interface [38]. The reduction of a TiO_2 surface is enhanced by spilled-over hydrogen [39], which can act as an electron donor to the reduced TiO_x surface and correspondingly increase the TiO_2 conductivity [40]. Most studies have found little evidence for a significant induced electronic effect in the metal; for example, the absence of strong perturbations in CO and H_2 thermal desorption spectra for model Pt/TiO_2 catalysts argued against such an effect and demonstrated clearly that surface coverages of both CO and H_2 correlated inversely with titania surface coverage [41]. Calorimetric studies have shown no significant support effect upon the heat of adsorption for H_2 [42] and only a small decrease in the heat of adsorption for CO on Pt/TiO_2 (HTR) catalysts [43]. The use in this study of large Pt crystallites with bulk electronic properties essentially unchanged by the TiO_x discounts variations in the Fermi level of the metal as an explanation for the enhanced activity. Thus, a geometric (or ensemble) effect, coupled with the formation of unique interfacial active sites, appears to be the principal factor in the metal–support interaction in the Pt–TiO_x system.

During both CO_2–CH_4 reforming and CO hydrogenation to CH_4, the gas-phase species to which the catalyst surface is exposed are identical, though in different concentrations. To our knowledge, no studies have been reported in the literature which investigated the role and stability of Ti^{3+} centers during CO_2–CH_4 reforming; thus, analysis of data reported for CO hydrogenation to CH_4 is of interest. Raupp and Dumesic [44], Wang et al. [45], and Tanaka et al. [33] have shown that H_2O and CO_2 dissociation involve the oxidation of Ti^{3+} to Ti^{4+}, and Bonneviot and Haller [38] have shown that CO irreversibly titrates Ti^{3+}. Regardless, Demmin et al. have shown that Ti^{3+} species are present under reaction conditions during CO hydrogenation to CH_4 [41] and Dwyer et al. have demonstrated that catalyst deactivation in this reaction correlates with a decrease in the concentration of Ti^{3+} centers [36]. A redox-type of mechanism has been proposed for Ti^{3+}–Ti^{4+} centers at the metal–support interface [44]. Alternatively, Wang et al. have recently shown that adsorbed HCOO species on reduced titania do not significantly oxidize Ti^{3+}, but block adsorption of H_2O and O_2 thereby preventing oxidation of Ti^{3+} [45]. The presence of CH_xO species on the support and in the metal–support interfacial region has been postulated during the CO_2 reforming of CH_4 [3] as well as during CO hydrogenation to CH_4 [46]. In the case of Pt/Al_2O_3, it is likely that these CH_xO species are stabilized via an interaction with exposed Al cations on the support surface [47]. Thus, if CH_xO species behave analogously to HCOO on reduced titania, it is highly probable that the presence of Ti^{3+} during CO_2–CH_4 reforming as well as CO hydrogenation to CH_4 is due to the formation of metastable CH_xO species at Ti^{3+} centers located in the metal–support interfacial region; i.e., the promoting effect of TiO_x may be related in part to the availability of Ti^{3+} centers. However, we can offer no direct confirmation that Ti^{3+} active centers exist at the metal–support interface during CO_2–CH_4 reforming over TiO_x/Pt.

5. Summary

The role of metal–support interactions in CO_2 reforming of CH_4 over Pt catalysts has been explored using model TiO_x/Pt catalysts. Through a combination of activity measurements and TPH of surface carbon, it has been shown that TiO_x species on the surface of Pt powder can suppress carbon deposition via a geometric effect, in which large ensembles of Pt atoms are destroyed by the presence of TiO_x species, and increase activity, presumably due to highly active sites in the metal–support interfacial region. In addition, it seems that CO_2–CH_4 reforming reaction over Pt can appear to be structure sensitive, but this behavior may be attributable to the extent of carbon deposition that can rapidly form. This topic can be more rigorously tested by investigating CO_2–CH_4 reforming over different single-crystal surfaces of Pt.

Acknowledgement

The authors would like to thank NEDO, a Japanese international joint research program, for sponsoring this study, the US Department of Education for providing a GAANN fellowship, and the NSF for an equipment grant (CTS-9311087) used to acquire the DRIFTS system.

References

[1] M.C.J. Bradford and M.A. Vannice, Appl. Catal. A. 142 (1996) 73, 97.
[2] Z.Zhang and X.E. Verykios, Appl. Catal. A 138 (1996) 109.
[3] M.C.J. Bradford and M.A. Vannice, J. Catal. (1997), in press.
[4] A. Erdöhelyi, K. Fodor and F. Solymosi, Stud. Surf. Sci. Catal. 107 (1997) 525.
[5] Z. Zhang, V.A. Tsipouriari, A.M. Efstathiou and X.E. Verykios, J. Catal. 158 (1996) 51.
[6] A. Erdöhelyi, J. Cserényi and F. Solymosi, J. Catal. 141 (1993) 287.
[7] O. Yamazaki, T. Nozaki, K. Omata and K. Fujimoto, Chem. Lett. 10 (1992) 1953.
[8] E. Ruckenstein and Y.H. Hu, Appl. Catal. A 133 (1995) 149.
[9] A.M. Gadalla and M.E. Sommer, J. Am. Ceram. Soc. 72 (1989) 683.
[10] J.T. Richardson, B. Turk and M.V. Twigg, Appl. Catal. A 148 (1996) 97.
[11] Y. Chen and J. Ren, Catal. Lett. 29 (1994) 39.
[12] A. Erdöhelyi, J. Cserényi, E. Papp and F. Solymosi, Appl. Catal. A 108 (1994) 205.
[13] A.M. Efstathiou, A. Kladi, V.A. Tsipouriari and X.E. Verykios, J. Catal. 158 (1996) 64.
[14] (a) M.A. Vannice and D. Poondi, J. Catal., submitted.
(b) D. Poondi, PhD Dissertation, The Pennsylvania State University, USA (1996).
[15] B.D. Cullity, *Elements of X-ray Diffraction*, 2nd Ed. (Addison-Wesley, Reading, 1978).
[16] J.W. Edington, *Practical Electron Microscopy in Materials Science* (N.V. Philips Gloeilampenfabrieken, Eindoven, 1976).
[17] R.K. Brandt, M.R. Hughes, L.P. Bourget, K. Truszkowska and R.G. Greenler, Surf. Sci. 286 (1993) 15.
[18] J. Segner, C.T. Campbell, G. Doyen and G. Ertl, Surf. Sci. 138 (1984) 505.
[19] G. Ertl, M. Neumann and K.M. Streit, Surf. Sci. 64 (1977) 393.
[20] J.R. Rostrup-Nielsen and J.-H. Bak Hansen, J. Catal. 144 (1993) 38.
[21] M. Boudart, Chem. Rev. 95 (1995) 661.
[22] J.M. Herrmann, M. Gravelle-Rumeau-Maillot and P.C. Gravelle, J. Catal. 104 (1987) 136.
[23] B.Z. Nikolic, H. Huang, D. Gervasio, A. Lin, C. Fierro, R.R. Adzic and E.B. Yeager, J. Electroanal. Chem. 295 (1990) 415.
[24] A. Rodes, E. Pastor and T. Iwasita, Anal. Quim. 89 (1993) 458.
[25] M.C. Román-Martínez, D. Cazorla-Amorós, C. Salinas-Martínez de Lecea and A. Linares-Solano, Langmuir 12 (1996) 379.
[26] C.R. Prichard and C.N. Hinshelwood, J. Chem. Soc. 127 (1925) 806.
[27] G.A. Somorjai, R.W. Joyner and B. Lang, Proc. Roy. Soc. London 331 (1972) 335.
[28] T.P. Beebe Jr., D.W. Goodman, B.D. Kay and J.T. Yates Jr., J. Chem. Phys. 87 (1987) 2305.
[29] D.J. Trevor, D.M. Cox and A. Kaldor, J. Am. Chem. Soc. 112 (1990) 3742.
[30] R. van Hardeveld and F. Hartog, Surf. Sci. 15 (1969) 189.
[31] M.F. Mark and W.F. Maier, J. Catal. 164 (1996) 122.
[32] M. Sigl, M.C.J. Bradford, H. Knözinger and M.A. Vannice, Topics Catal., submitted.
[33] K. Tanaka, K. Miyahara and I. Toyoshima, J. Phys. Chem. 88 (1984) 3504.
[34] W. Fancheng, W. Huilin, K.R. Tsai, W. Shuijuand and X. Fuchun, Catal. Lett. 12 (1992) 319.
[35] U. Bardi, K. Tamura and Y. Nihei, Catal. Lett. 3 (1989) 117.
[36] D.J. Dwyer, J.L. Robbins, S.D. Cameron, N. Dudash and J. Hardenbergh in: *Strong Metal Support Interactions*, ACS Symposium Series 298 (Am. Chem. Soc., Washington, 1986) p. 21.
[37] A.A. Davydov, M.P. Komarova, V.F. Anufrienko and N.G. Maksimov, Kinet. Catal. 14 (1973) 1342.
[38] L. Bonneviot and G.L. Haller, J. Catal. 113 (1988) 96.
[39] X.S. Li, W.Z. Li, Y.X. Chen and H.L. Wang, Catal. Lett. 32 (1995) 31.
[40] U. Roland, R. Salzer, T. Braunschweig, F. Roessner and H. Winkler, J. Chem. Soc. Faraday Trans. 9 (1995) 1091.
[41] R.A. Demmin, C.S. Ko and R.J. Gorte, J. Phys. Chem. 89 (1985) 1151.
[42] B. Sen, P. Chou and M.A. Vannice, J. Catal. 101 (1986) 517.
[43] M.A. Vannice, L.C. Hasselbring and B. Sen, J. Catal. 97 (1986) 66.
[44] G.B. Raupp and J.A. Dumesic, J. Phys. Chem. 89 (1985) 5240.
[45] L-Q. Wang, A.N. Shultz, D.R. Baer and M.H. Engelhard, J. Vac. Sci. Technol. A. 14 (1996) 1532.
[46] B. Sen and J.L. Falconer, J. Catal. 125 (1990) 35.
[47] J.L. Robbins and E. Marucci-Soos, J. Phys. Chem. 93 (1989) 2885.
[48] M.A. Vannice and C. Sudhakar, J. Phys. Chem. 88 (1984) 2429.